Chapter II

Literature Survey

Deformation Behaviour during Hot Deformation

The mechanical properties of steel sheet depend mainly on the microstructure, i.e., grain size and precipitation state. The microstructural evolution is strongly affected by several processes during deformation, which

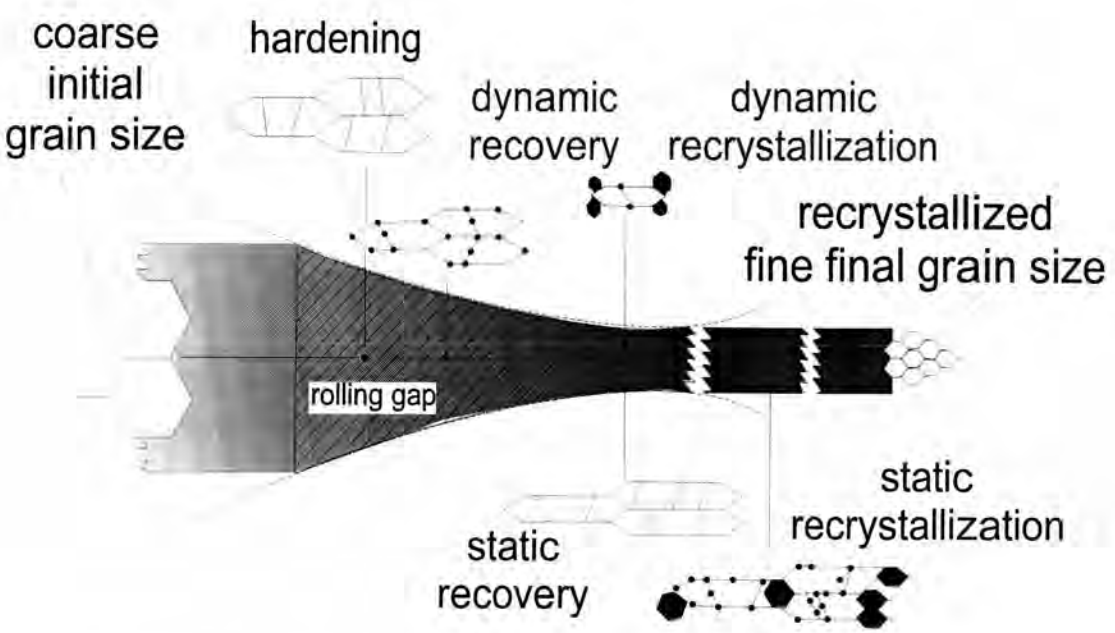

Fig. 2-1 : Schematic illustration of the softening processes and their influence on the development of austenite structure during hot rolling of steels (Dahl et al., quoted in Biegus, Kaspar and Lotter [2])

means hardening and softening processes such as precipitation, recrystallization or recovery.

Deformation behaviour during hot rolling in the austenitic range, which lead to grain refinement as shown in figure 2-1. During hot rolling, work hardening takes place similar to an increase in dislocation density. This results in a strained austenite structure. If the deformation or strain reaches a certain value, dynamic softening process starts, i.e., recovery or recrystallization. This results in a decreasing dislocation density, if the rate of work hardening is lower than the rate of dynamic softening processes. Even after deformation or between different deformation steps, softening processes may still occur, if a certain strain value or dislocation density is reached a certain value. Static softening processes, i.e., recovery and recrystallization as well as dynamic softening processes lead either to substructure formation or growing of new grains, which results in a finer microstructure compared to the initial grain size.

The following topics will give a short overview about dynamic and static softening processes.

Dynamic Softening

Flow curves of hot deformation can be classified as shown in figure 2-2.

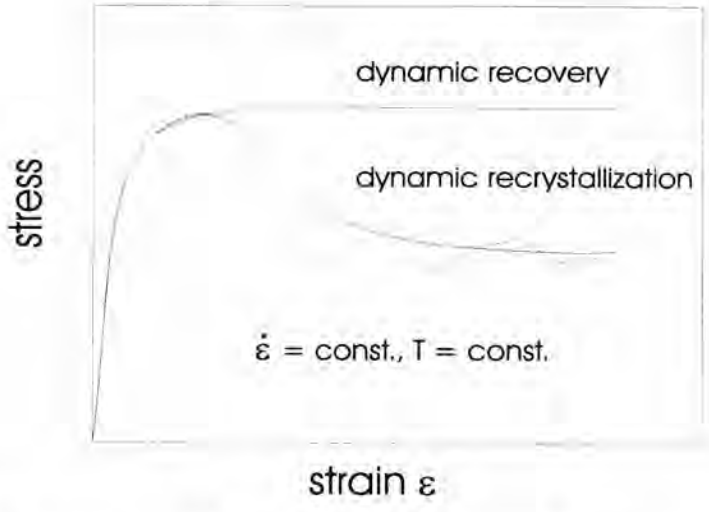

Fig. 2-2 : Different types of hot flow curve (Böhme, Hensger and Klimanek [3])

In the flow curve of dynamic recovery, the stress increases with increasing strain at the beginning part, due to the fact that the rate of work hardening is higher than the rate of softening by dynamic recovery. After that, the flow curve reaches a steady state, that the rate of work hardening equal to the rate of softening by dynamic recovery. In the flow curves of dynamic recrystallization, the stress also increases with increasing strain at the beginning part similar to the flow curve of recovery. When the strain reaches a certain value, dynamic recrystallization starts. After that, the stress is decreasing due to the rate of softening by dynamic recrystallization is higher than the rate of work hardening. The flow stress reaches a steady state stress with a characteristic peak. This is different from the flow curve of dynamic recovery. At high temperature and low strain rate the flow curve of dynamic recrystallization has a cyclic shape after the maximum peak.

Dynamic recrystallization is the formation of new grains in the deformed matrix of material during deformation. Biegus et al. [2] described that the kinetics of recrystallization depend either on the steel grade, e.g., chemical composition, initial grain size, precipitation status, content of inclusion, and also on the deformation or process parameters, such as temperature, strain, strain rate and deformation sequence.

The influence of dynamic recrystallization on the flow stress and the microstructural evolution are schematically shown in figure 2-3 and 2-4, respectively. The flow stress is considered as a value to calculate or describe the force needed for a certain deformation. The flow stress values are a function of the work hardening and softening processes during deformation, which may be used to describe them.

Figure 2-3 shows a typical curve for dynamic recrystallization. Normally dynamic recrystallization starts at a certain strain value (ε_c) before the strain at the maximum stress. This critical strain value is similar to a certain dislocation density, which is required to start recrystallization. In the fact that recrystallization means the formation of new grains, the energy for the formation of recrystallization nuclei as well as the growth of those nuclei has to be supported by the material. This is possible if the critical dislocation density is reached, because dislocations, i.e., the distortion of the atomic structure are

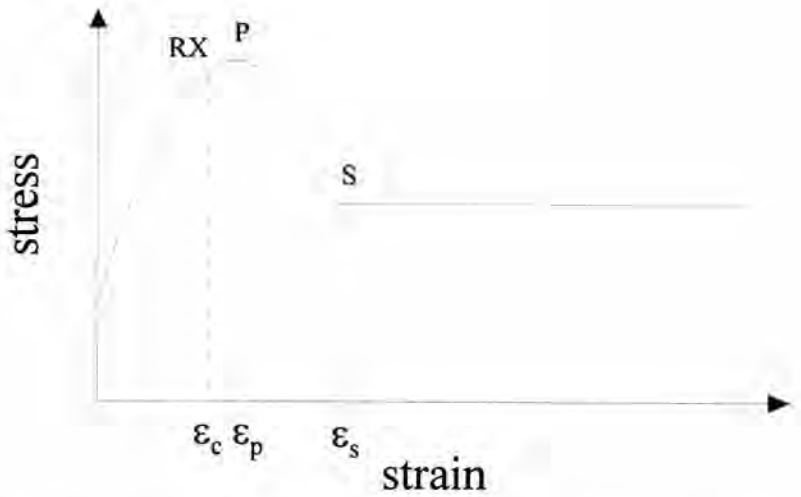

Fig. 2-3 : Stress as a function of dynamic recrystallization

similar to an energy reservoir, which is used for the formation of recrystallization nuclei and followed by a microstructure with a lower energy potential.

The value of the so called critical strain (ε_c) is also a function of the dynamic recovery process which occurs after the deformation starts. Although recovery does not lead to a formation of new grains, the number of dislocations is reduced due to annihilation and polygonization processes followed by the formation of a subgrain structure.

When deformation starts the number of dislocation is increasing due to work hardening. At the same time dynamic recovery leads to a lower dislocation density, work hardening still predominates until the critical value of ε_c is reached and recrystallization starts. Sellars [4] stated that the critical strain

of C-Mn steels may be approximated as a constant fraction (0.8) of the strain at the peak stress.

$$\varepsilon_c = 0.8\ \varepsilon_p \qquad \text{(Equation 1)}$$

Figure 2-4 schematically describes the different states during dynamic softening and their effect on the microstructure. At strains less than ε_c the rate of work hardening is higher than the rate of softening by dynamic recovery, the dislocation density increases with the strain. Grains are elongated before they are gradually polygonizing to subgrains (Hernandez and Medina [5]). In the strain range between the critical strain (ε_c) and the strain at peak stress (ε_p) dynamic recrystallization occurs. However the flow stress still increases up to

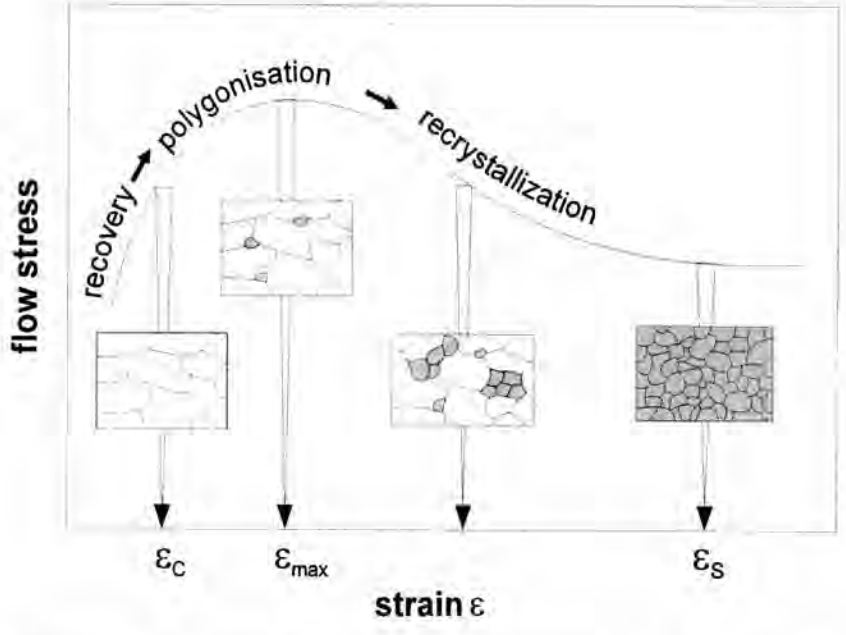

Fig. 2-4 : Microstructural evolution due to dynamic recrystallization (Böhme et al. [3])

a maximum due to a rate of work hardening higher than the rate of softening by dynamic recrystallization. In the strain range between the strain at peak stress (ε_p) and the strain at steady stress (ε_s) the material is softening due to a rate of dynamic recrystallization higher than the rate of work hardening. The strain range between the critical strain (ε_c) and the strain at steady state stress (ε_s) is the range of partially dynamic recrystallization. The strain range after ε_s is the range of steady state dynamic recrystallization, where the formation of new dislocations due to work hardening is equivalent at a certain value to the reduction of dislocation density due to dynamic recrystallization (Tamura [6]), whereby the mean grain size becomes constant. The grain size depends only on the stress at steady state $<\sigma_s>$ (Luton and Sellars, quoted in Hernandez and Medina [5]).

Chemical composition is a parameter, which has an influence on flow curves. Figure 2-5 shows the effect of alloying element on the changing of flow stress. In this figure, the deformation temperature at 1000 °C and a constant strain rate of 1.0/s were used. The flow stress is considered at a strain of 0.1. Co, V, Cr, Ni, Mn and C are the elements, which increase the flow stress in the usual composition range. In this composition range, increasing content of Nb, Si, or W results in the reduction of flow stress. Increasing content of Ti or Al increases the flow stress as shown at the beginning of this curve. However, after alloying with a certain amount, still increasing contents

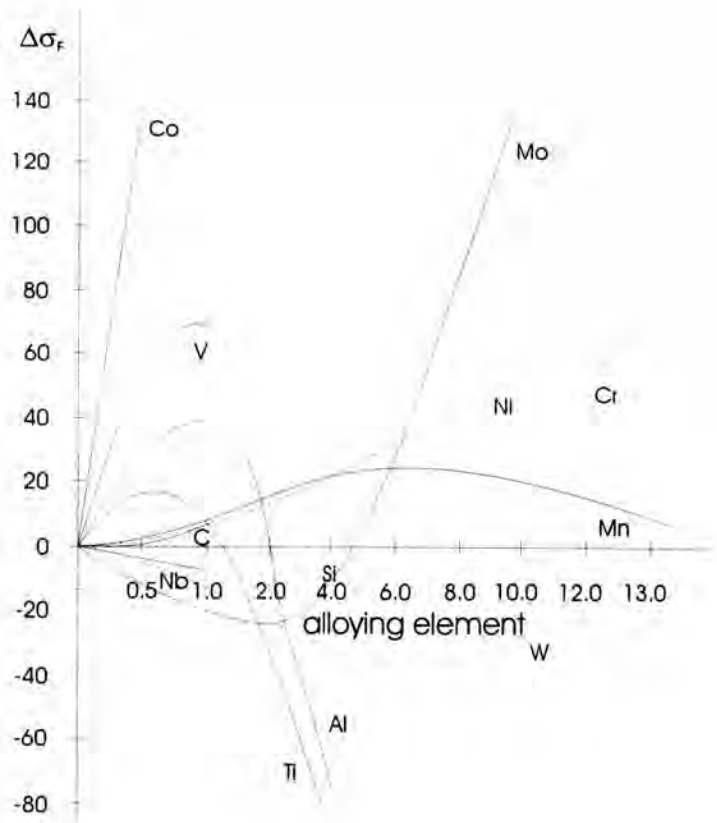

Fig. 2-5 : Effect of alloying elements on the changing of flow stress compared to pure iron <deformation temperature T_d = 1000°C, ε = 0.1 and $\dot{\varepsilon}$ = 1.0/s> (Spittel and Spittel [7])

of this element results in the decreasing of flow stress. In the opposite increasing content of Mo decreases the flow stress as shown at the beginning of this curve. After alloying with a certain amount, still increasing content of this element results in the increasing of flow stress.

Flow curves of microalloyed steel are different from flow curves of unalloyed steel. The yield stress and critical strain of microalloyed steel are

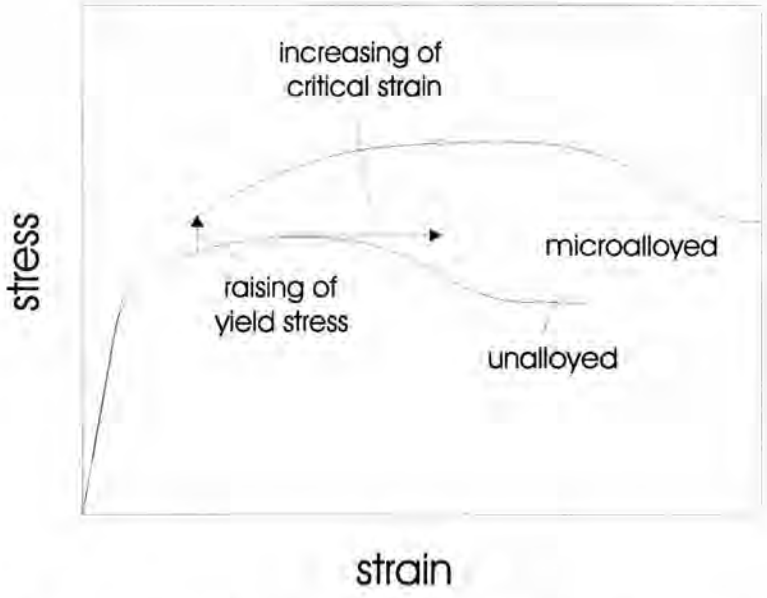

Fig. 2-6 : Hot flow curves of unalloyed and microalloyed steel (Meyer [8])

higher than those of unalloyed steel as shown in figure 2-6. This difference may result from precipitation effects.

Figure 2-7 shows the effect of deformation temperature and strain rate on critical flow stress of IF steel after austenitizing at 1250 °C for 10 minutes. Critical flow stress (S_{crit}) means the equivalent stress for initiation of dynamic softening, can be evaluated and equals to the stress at critical strain. The critical strain was calculated by equation 1. In addition, the critical strain is an analogy with the required for the initiation of conventional static recrystallization. From figure 2-7, the critical flow stress either in the austenitic range or in the ferritic range increases with decreasing deformation temperature. Phase transformation from the austenite to ferrite causes a relative minimum of flow stress suggesting that rolling torque could be reduced by rolling the steel in ferrite range. The

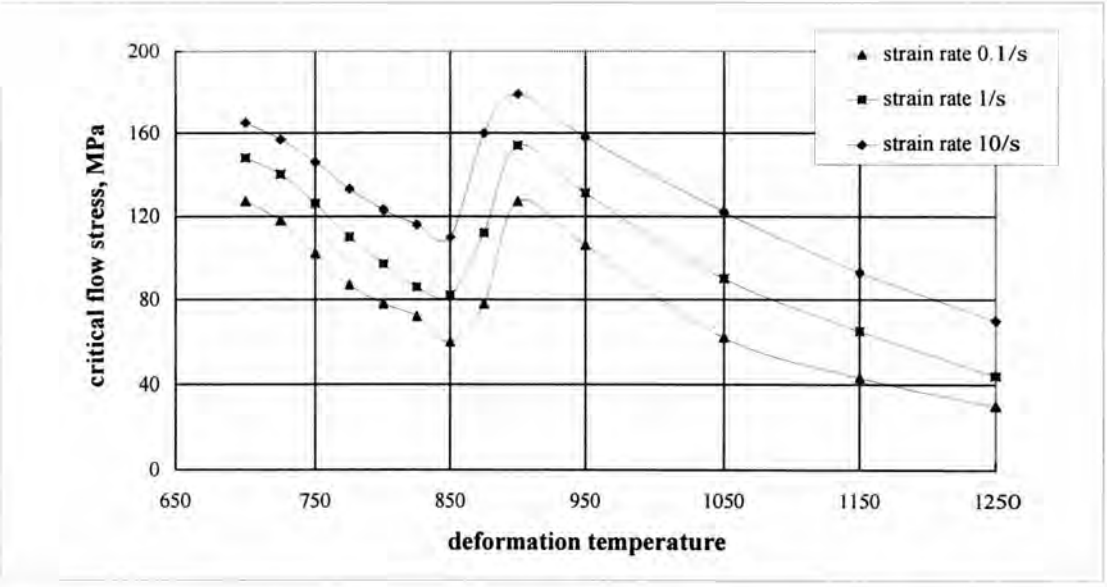

Fig. 2-7 : Effect of deformation temperature and strain rate on the critical flow stress of IF steel after austenitizing at 1250 °C for 10 minutes

Chemical composition in wt% of IF steel : 0.002 C, 0.13 Mn, 0.036 Al, 0.08Si, 0.0033 N and 0.056 Ti (Bleck, [9])

maximum and minimum of critical flow stress of this steel is almost constant regardless the strain rate.

The flow curve and microstructure particularly depend on the temperature and the strain rate. In the temperature range where no precipitation or transformation reactions occur, those parameters can be combined in terms of the Zener-Hollomon parameter (Z) as

$$Z = \dot{\varepsilon} \exp(Q_{def}/RT) \qquad \text{(Equation 2)}$$

where Q_{def} is the activation energy for deformation.

For C-Mn steels the equation 2 can be rewritten to (Sellars [4])

$$Z = \dot{\varepsilon} \exp(312000/RT) \qquad \text{(Equation 3)}$$

The strain at the peak stress (ε_p) is a function of initial grain size (d_0) and Z as the following equation shows

$$\varepsilon_p \propto d_0^{a1} Z^{a2} \qquad \text{(Equation 4)}$$

where a_1 and a_2 are constants, then

$$\varepsilon_p = 6.97\times10^{-4} d_0^{0.3} Z^{0.17} \qquad \text{(Equation 5)}$$

for C-Mn steels where d_0 is expressed in μm (Sellars [4]).

According to the equation 5, the strain at the peak stress increases with increasing value of Z and with increasing initial grain size.

Karhausen, Kopp, and Souza [10] stated that the strain at steady stress is a function of initial grain size (d_0) and Z and may be described by the following equation.

$$\varepsilon_s = a_3.\varepsilon_p + a_4.Z^{a5} \qquad \text{(Equation 6)}$$

where a_3, a_4 and a_5 are constants.

Karhausen et al. also stated that the peak stress is only a function of Z as

$$\sigma_p = a_6.Z^{a7} \qquad \text{(Equation 7)}$$

where a_6 and a_7 are constants.

In 1988, Hirano et al. [11] found that the dynamically recrystallized grain size (d_{dyn}) does not depend upon the initial grain size and is independent of effective strain. It is only a function of the stress at steady state (Hernandez, and Medina [5]; Karhausen and Kopp [12]). The stress at steady state of dynamic recrystallization is only a function of Z as follows (Sellars [13])

$$\sigma_s \propto Z^{a8} \qquad \text{(Equation 8)}$$

where $a_8 = 0.1\text{-}0.2$.

According to the equation 5, 6, 7 and 8, σ_p, ε_p, σ_s and ε_s are increasing with higher value of Z

Figure 2-8 shows the effect of austenite grain size before deformation on the stress-strain curves at the same value of Z. The strain at peak stress in case of coarse austenite grain is higher than that in case of fine austenite grain.

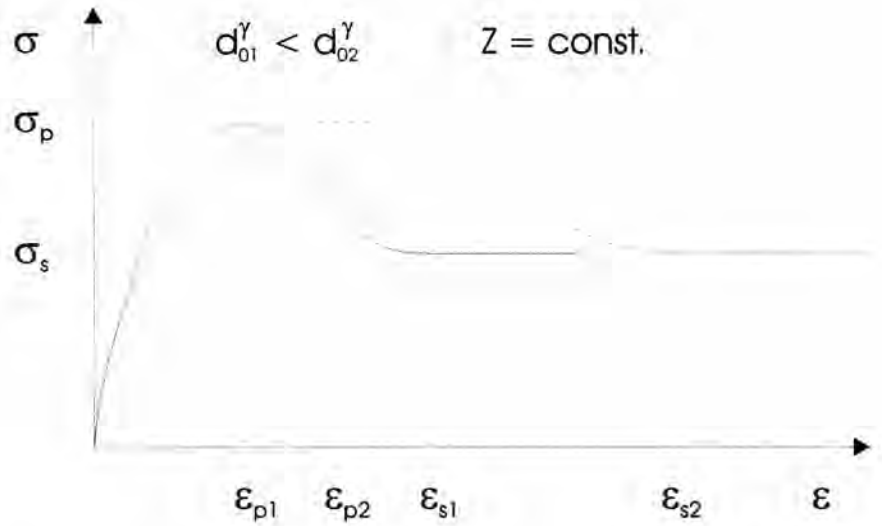

Fig. 2-8 : Effect of austenite grain size on stress-strain curves (Bourell and McQueen, quoted in Karhausen et al [10])

This results from the high work hardening rate of fine grain size (Brimacombe et al. [14]). The dislocation density in case of fine grain reaches the critical strain at lower values than that in case of coarse grain. Therefore fine austenite grain promotes dynamic recrystallization. At the same value of Z, the peak stress and steady state stress are almost the same value in both flow curves.

A formulation for determination of flow stress was developed by Cingara, Germain and McQueen (quoted in Karhausen and Kopp [12]).

$$\frac{\sigma}{\sigma_p} = \frac{\varepsilon}{\varepsilon_p}.(\exp(1-\frac{\varepsilon}{\varepsilon_p}))^{a9} \qquad \text{(Equation 9)}$$

where a_9 is a constant.

For C-Mn steels dynamically recrystallized fraction according to Avrami's law has the following form (quoted in Karhausen et al. [10])

$$X_{dyn} = 1\text{-}\exp[a_{10}.[(\varepsilon\text{-}\varepsilon_c)/(\varepsilon_s\text{-}\varepsilon_c)]^{a11}] \qquad \text{(Equation 10)}$$

or (quoted in Hernandez, and Medina [15])

$$X_{dyn} = 1 - \exp[-a_{12}.(\frac{\varepsilon - a_{13}\varepsilon_p}{\varepsilon})^{a14}] \qquad \text{(Equation 11)}$$

$$\varepsilon > a_{13}\varepsilon_p$$

where a_{10}, a_{11}, a_{12}, a_{13}, a_{14} are constants, $0< a_{12} <1$; $1< a_{14} <2$ and $(a_{13}\varepsilon_p)$ is equal to the critical strain.

In 1987, Tamura [6] proposed that the average size ($\bar{d}_{dyn}$) of dynamically recrystallized grains is only a function of Z as follows

$$\bar{d}_{dyn} = a_{15}Z^{-a16} \qquad \text{(Equation 12)}$$

where a_{15} and a_{16} are material constants and a_{16} is about 0.3-0.4 for all steels.

From equation 12, dynamically recrystallized grain size increases as Z decreases, e.g., increasing strain rate or decreasing deformation temperature.

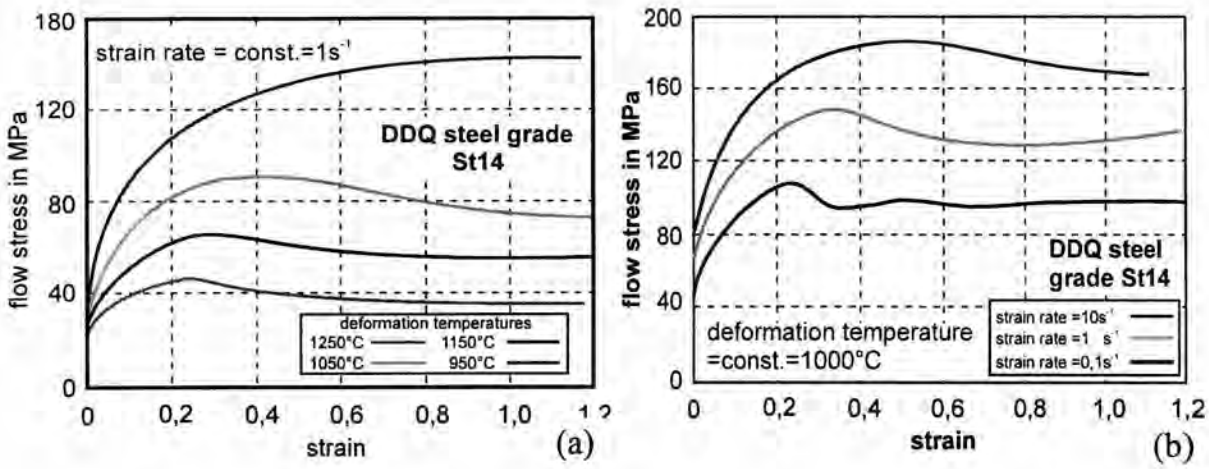

Fig. 2-9 : (a) Influence of temperature on the flow curves of IF steel

(b) Influence of strain rates on the flow curves of IF steel

Chemical composition in wt% of St 14 : 0.048 C, 0.24 Mn, 0.047 Al, 0.01Si, 0.0036 N, 0.008 P, 0.009 S, 0.15 Cu, 0.023 Cr and 0.019 Ni (Groβheim [16])

Figure 2-9 (a) and (b) show the effect of temperature and strain rate on flow curve of IF steel. Increasing temperatures or decreasing strain rates result in low flow stress values, whereby the peak stress and the onset of the steady range (point s in figure 2-3) are shifted towards smaller strains. Decreasing temperature or increasing strain rates delay the onset of the recrystallization followed by an incompletely recrystallized microstructure (Hernandez and Medina [15]).

Hernandez and Medina also demonstrated that when the strain rate is very low, with values of 0.01 s^{-1} or less, and the temperatures are high, periodic recrystallization may appear and the flow curve will show multiple peaks as

shown in figure 2-9 (b). But in hot rolling the strain rate applied in each pass is greater than that mentioned above, therefore the periodic recrystallization does not occur in real processes.

In 1984, Jonas and Sakai [17] demonstrated that multiple peak flow curves are associated with grain coarsening. and single peak flow curves are associated with grain refinement. With increasing strain rate the flow curve displays a single peak, whereas with decreasing strain rate multiple peaks are observed.

Figure 2-10 shows the progress of dynamic recrystallization in case of grain refinement. It can be seen that the first nuclei for new grains occur at grain boundaries followed by a ''necklace'' structure. Subsequent nucleation occurs preferentially at the interface between the existing necklace and the remaining part of original grain. This leads to a ''cascade'' of nucleation. Before recrystallization is complete, the first formed necklace grains may reach their critical strain and recrystallize again.

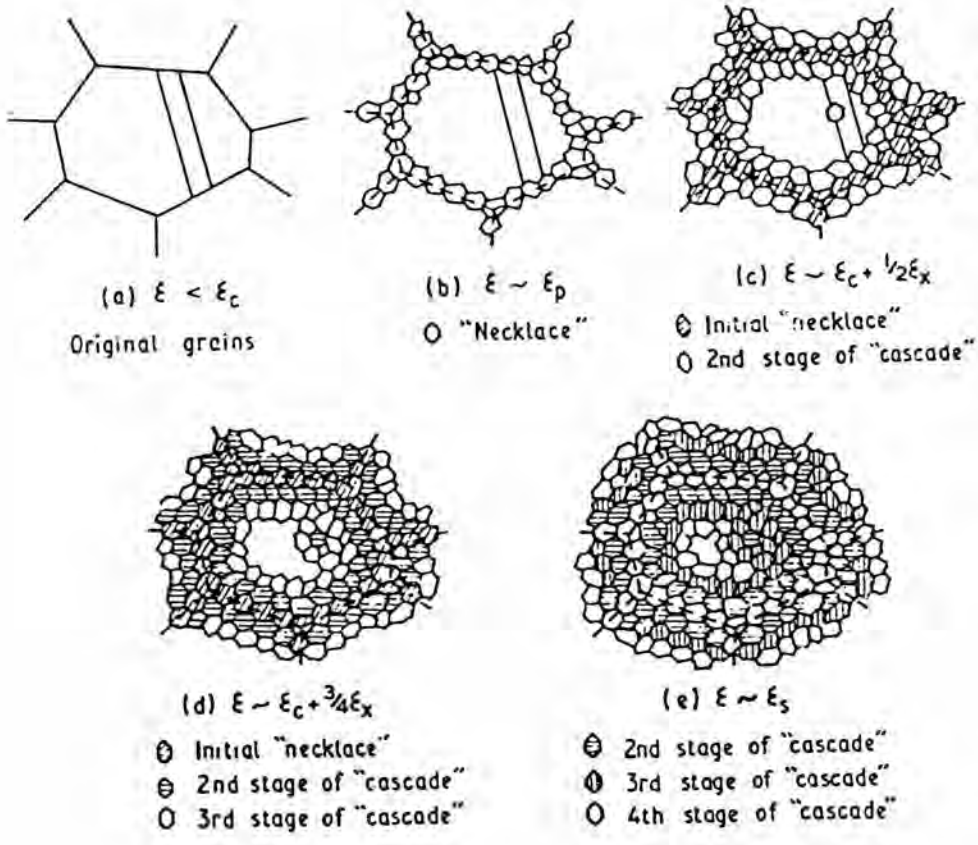

Fig. 2-10 : Schematic illustration of the progress of dynamic recrystallization when the recrystallized grain size is much smaller than the original grain size (Sellars [13])

Stüwe [18] stated that the microhardness of a partly recrystallized matrix is low in some places and high in others. This is different from recovery, where no new grains are formed and softening occurs homogeneously everywhere in the matrix. Therefore the microhardness of a partly recovered matrix is lowered everywhere.

Sakai, Xu and Zhang [19] stated that dynamic recrystallization is not the only mechanism in the conventional hot rolling, because the pass strains as well as the accumulated strains are usually smaller than the critical strain for initiating dynamic recrystallization.

Static Softening

Static softening is a combination of recovery, recrystallization and grain growth. These mechanisms occur during interpass time between 2 deformation passes or after one deformation step. In addition, these mechanisms may interfere with strain induced precipitation (Gabrovsek, Vodopivec, and Zvokelj [20]).

Static recrystallization is the nucleation of new grains in the deformed matrix of the material after deformation, e.g., during interpass time. Recrystallization process after deformation can be divide by an incubation time for nuclei formation into static recrystallization and metadynamic recrystallization. Static recrystallization needs a certain time for for nuclei formation, while metadynamic recrystallization occurs immediately after deformation.

During deformation with low strains associated with low dislocation density only dynamic recovery occurs, subsequent softening after deformation

is due to static recovery. Higher strains and dislocation densities may lead to additional softening due to static recrystallization.

However different models have been published to describe static softening mechanisms, in case that partial or complete recrystallization has occurred during deformation. The model of Djaic and Jonas is shown in figure 2-11. According to this model, static softening is a function of time and can be divided by subsequent processes into static recovery, metadynamic recrystallization and static recrystallization. These processes are affected by the previous dynamic softening processes. Strain values above ε_c, lead to static recovery, static recrystallization as well as metadynamic recrystallization. Long annealing times after static softening may lead to additional softening by grain coarsening.

The statically recrystallized fraction during isothermic annealing after hot deformation according to the Avrami equation is (quoted in Beynong, McLaren, and Sellars [22])

$$X_s = 1 - \exp[1-(\ln 2)(t/t_{0.5})^{a17}] \qquad \text{(Equation 13)}$$

where X_s is the recrystallized volume fraction during the annealing time t and $t_{0.5}$ is the time for a recrystallized fraction of 50 % and a_{17} is a constant time exponent.

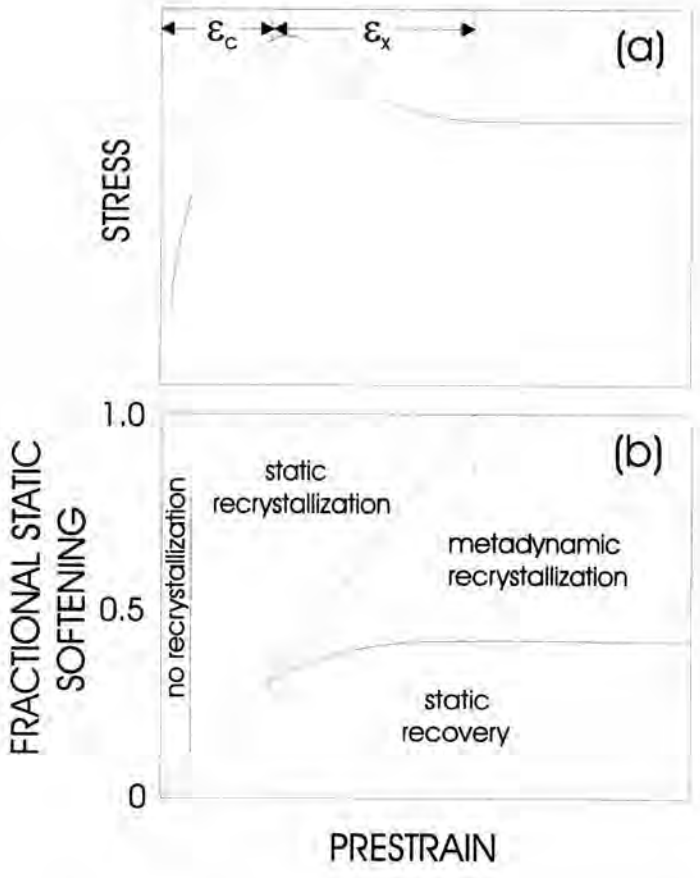

Fig. 2-11 : Relation between dynamic recrystallization (a) and static softening mechanisms (b) as a function of strain (Djaic and Jonas, quoted in Sellars and Whiteman [21])

Sellars [23] stated that the kinetic of recrystallization depends on deformation parameters as follows

$$t_{0.5} = f(d_o\,,\ \varepsilon,\ Z)\ \exp\ Q_{rex}/RT \qquad \text{(Equation 14)}$$

where Q_{rex} is the activation energy for recrystallization, ε is the prior strain and Z is the Zener-Hollomon parameter for the previous deformation.

Sellars also stated that in the temperature range without precipitation reactions, Q_{rex} is generally found to be constant, depending only on the chemical composition of the steel.

The statically recrystallized grain size is different from the dynamically recrystallized one, since the statically recrystallized grain size d_r depends on initial grain size, d_0, which is an index for the number of nuclei for recrystallization, as the following equation (Biegus et al. [2])

$$d_{rex} = a_{18} \cdot d_o^{a19} \cdot \varepsilon^{a20} \cdot \exp(Q_d/RT) \qquad \text{(Equation 15)}$$

The values a_{18}, a_{19}, a_{20} and Q_d are material-specific constants.

This recrystallized grain size is achieved when recrystallization is just complete. When recrystallization is only partially complete, the current size of the recrystallized grain, d_r, is given by (Beynong et al. [22])

$$d_r = X^{1/3} d_{rex} \qquad \text{(Equation 16)}$$

where X is the recrystallized fraction, and d_{rex} is the completely recrystallized grain size.

With same initial grain size, softening is accelerated with rising deformation temperature and increasing strain rate. The grain structure after

static recrystallization is generally finer than the initial microstructure before deformation (Biegus et al. [2]).

However, Glover and Sellars [24] stated that the statically recrystallized grain sizes are much larger than the dynamically recrystallized ones and have a lower stress dependency, probably because nucleation occurs continuously during dynamic recrystallization but is complete at the start of static recrystallization.

After recrystallization, grain growth takes place as a function of time and temperature. Campbell et al. [25] stated that the kinetic of grain growth is given by an equation of the form

$$d^m = d_r^m + a_{21}.t \exp\{-\frac{Q_{gg}}{RT}\} \qquad \text{(Equation 17)}$$

where Q_{gg} is the activation energy for grain growth with a value of about 400 kJ/mol for C-Mn steels and a_{21} and m are constants with m-values between 6 and 10.

Sakai et al. [19] stated that the statically softened fraction after partial dynamic recrystallization and dynamic recovery increases with the carbon content because of the higher diffusion rate of vacancies.

The statically softening fraction is determined by evaluation of flow curves according to the so-called multi-stroke technique. The calculation formula for statically softening fraction is shown in figure 2-12, whereby E_{stat} is the statically softening fraction.

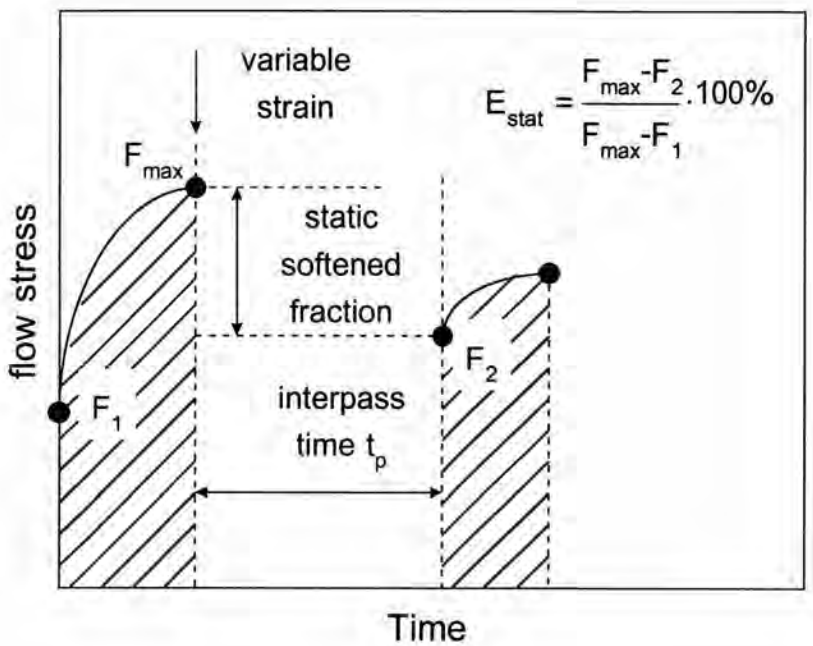

Fig. 2-12 : Multi-stroke technique to evaluate static softening processes

Dynamic recrystallization requires high reductions at low strain rate and high deformation temperatures, whereas static recrystallization is promoted by high reduction, high strain rate and high annealing temperature (Brimacombe et al. [26]).

Difference Between Austenite and Ferrite

As far as investigated, different softening mechanisms occur during deformations of austenite and ferrite. Because of its high stacking fault energy with values between 180 and 1450 mJm^{-2} (Hartley, quoted in Groheim [27]) and its body-centered cubic structure ferrite is expected to undergo dynamic recovery. Austenite is prone to dynamic or static recrystallization caused by its face-centered cubic structure and its low stacking fault energy of about 14 mJm^{-2} (Gallagher [28]). As investigations shown recrystallization processes during deformation become more important with decreasing stacking fault energy although recovery processes always occur. As reported in several studies above, recovery processes are a consequence of dislocation movements. Usually annealed material has a dislocation density of about 10^{10}-10^{11} m^{-2}. During deformation the dislocation density increases with the strain, i.e., 10^{11}-10^{12} m^{-2} at the beginning of macroscopic flow (Jonas and McQueen [29]), although annihilation processes lead to a decreasing number of dislocation. During strain hardening the dislocation density generation rate and the annihilation rate are increasing. Caused by the predominant generation of new dislocations the dislocation density is increasing until the steady state is reached. In the steady state the dislocation density is constant depending on the annihilation rate, which is a function of dislocation movements such as climbing, cross-slip, node and unpinning.

As well known, softening due to recrystallization processes can be led back to the decrease of dislocation density by nucleation and grain growth and a replacement of the strained structure by new formed grains. During recovery the number of dislocations is reduced by annihilation processes which lead to softening. During strain hardening the dislocation entangle or cellular substructures are formed. In the steady state all dislocations are arranged into subgrains with their grain size and orientation depending on the material itself, the deformation temperature and strain rate.

As dislocations can be moved more easily by climbing and cross slip in structures with high stacking fault energy similar to recovery processes, ferrite is considered to be prone to dynamic recovery, whereas mainly dynamic recrystallization occurs in the austenite. Recently it is reported that dynamic recrystallization can take place in commercial steel grades with carbon contents of 0.6-0.7 (Gohda, Hashimoto and Watanabe [30]). Static recrystallization may occur either in austenite or in ferrite, although static recrystallization of austenite is initiated by a minimum strain of about 10 %, whereas ferrite requires at least 60 % deformation per pass (Gabrovsek et al. [20]).

By mean of static softening the difference between austenite and ferrite can be seen in figure 2-13. Deformation in the austenite the main softening process is static recrystallization which occurs within a few seconds. For deformation in the ferritic range even interpass time of 50 seconds did not

lead to softening fractions above 50-60%. The softening in the ferrite is mainly a result of recovery processes.

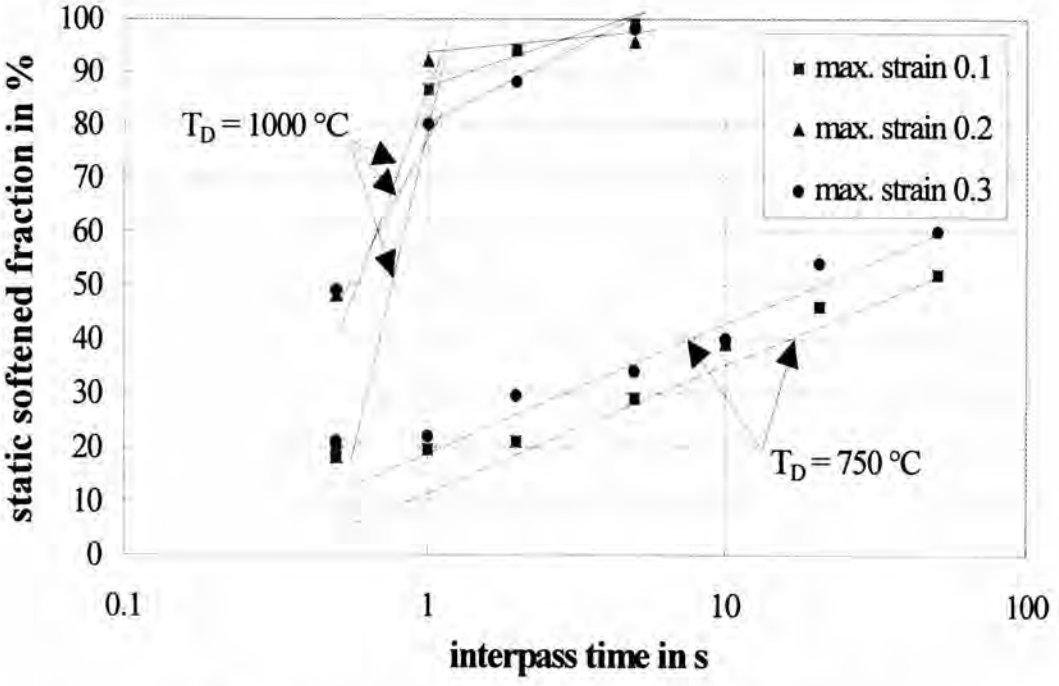

Fig. 2-13 : Static softening of VAC steel after deformation in austenite or ferrite

Chemical composition in wt% of VAC steel : 0.006 C, 0.22 Mn, 0.030 Al, 0.03Si and 0.005 N (Bleck, Feldhaus, and Gupta, [31])

Rolling Techniques

1 Rolling in Austenite Phase Austenitic rolling is defined as hot rolling where finishing rolling is performed at temperatures above A_{r3}. Normally the slab with a thickness of 200 to 250 mm is reheated at 1100 to 1250 °C for 2-3 hours (Jonas and McQueen [29]). Roughing rolling is

performed in 3-5 passes in a temperature range of 1200 to 1000°C. The intermediate slab with a thickness of about 45 mm is then transferred to finishing stands. After rolling to required thickness (typically less than 6 mm) the strip is air or water cooled to coiling temperature in the range of 750 to 550°C (Gabrovsek et al. [20]). New rolling techniques have been developed to improve the mechanical properties, e.g., recrystallized controlled rolling as well as thermomechanical control processing. Subsequent cold rolling is required to produce thin strips with a thickness less than 1.8 mm (Herman and Leroy [1]).

2. Rolling in Dual-phase Range (Intercritical Rolling) To produce steel sheets for drawing application, intercritical rolling is undesirable because its lead to reduced quality of the mill products such as poorer flatness, thickness inhomogeneities (Beco et al. [32]). Besides that, this rolling leads metallurgical defects such as abnormal grain growth, elongated ferrite structure as well as planar anisotropy of mechanical properties (Gohda et al. [30]).

3. Rolling in Ferrite Phase In ferritic rolling the hot rolling can either be finished in ferritic region or can be completely performed in the ferritic range as shown in figure 2-14. This rolling can control profile of product better than austenitic rolling, and requires lower rolling load than cold rolling.

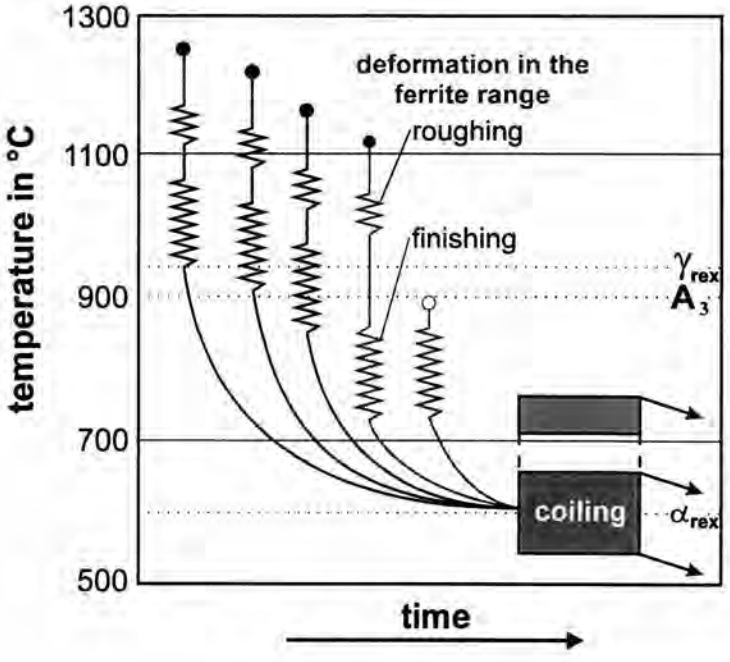

Fig. 2-14 : Processing schedules for austenite and ferrite (Bleck and Esser [33])

Herman and Messien [34] demonstrated that drawing quality of ferritic strips can be improved by optimized chemical composition (low carbon-low manganese), use of lubricants at the finishing stands as well as adjustment of cold rolling reduction.

Ferritic rolling is suitable for low carbon steel. The low carbon steel is critical to be rolled in austenite phase due to high transformation temperature and narrow temperature range of transformation, especially for extra low carbon and ultra low carbon. Especially when rolling for thin gauges, phase transformation may be occur and lead to poorer mechanical properties.

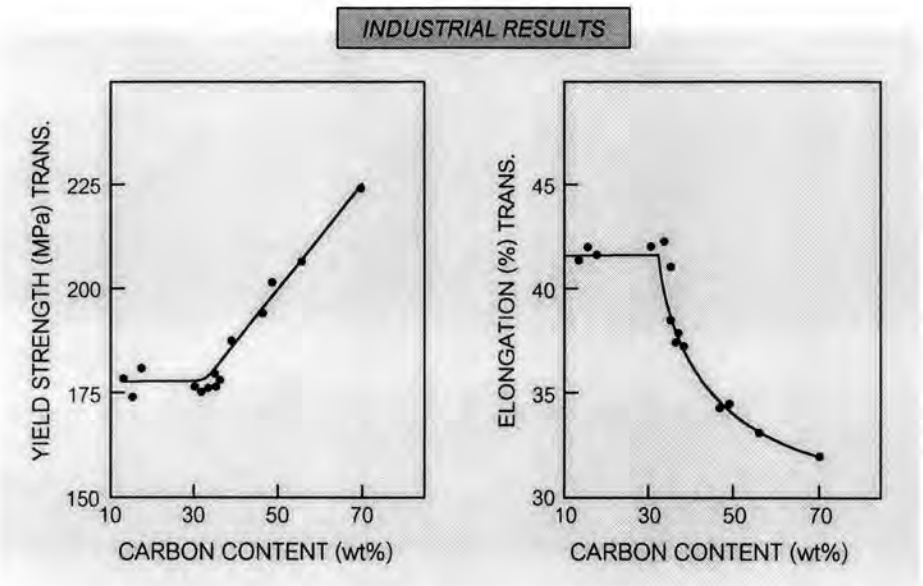

Fig. 2-15 : Influence of the carbon content on the transverse yield strength and ductility after ferritic rolling <finishing : 800-750 °C, coiling : 700-650 °C, thickness : 2-2.5 mm> (Herman and Leroy [1])

In ferritic rolling, the carbon content should be kept below 0.04 wt%, in order to avoid any intercritical rolling as shown in figure 2-15. By this, the ferritic hot strips will have low yield strength and high elongation with suit for drawing application.

The influence of processing temperature on the mechanical properties of Ti-Nb IF steel are shown in figure 2-16 (a) and 2-16 (b). For rod rolling applications, low strength values in combination with high elongation values are required. It can be seen very clearly that finishing temperatures between 700 and 850 °C lead to lower strength and higher elongation values than rolling in the austenitic range.

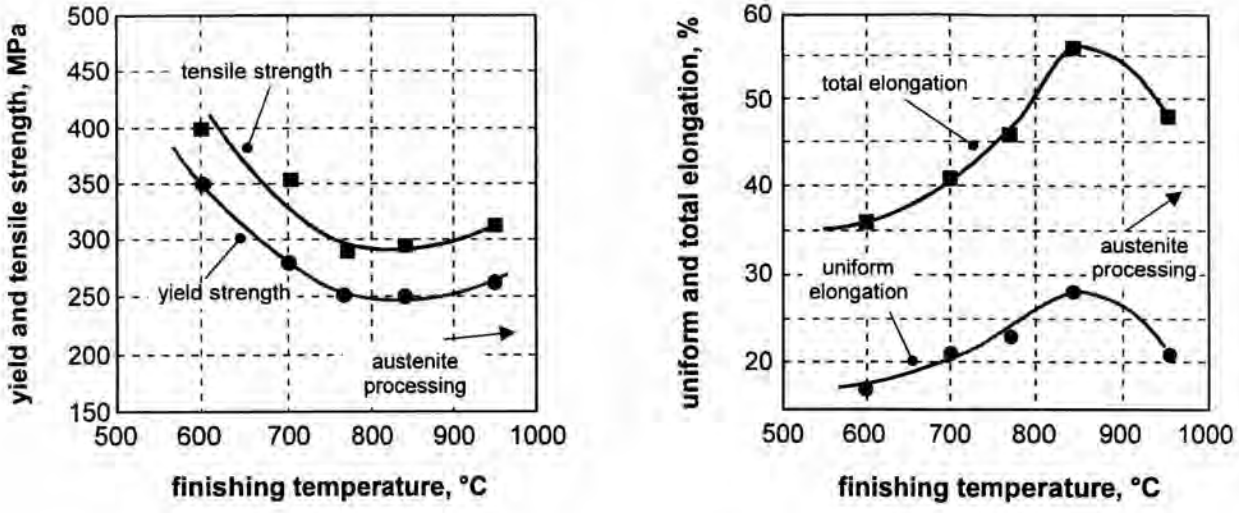

Fig. 2-16 : (a) Effect of deformation temperature on yield and tensile strength

(b) Effect of processing temperature on uniform and total elongation

Chemical composition in wt% of Ti-Nb IF steel : 0.003 C, 0.18 Mn, 0.054 Al, 0.003 P, 0.005 S, 0.0018 N, 0.018 Ti, 0.020 Nb (Cetlin, Jonas and Yue [35]).

Advantages of Ferritic Rolling

- energy saving up to 20% (Beco et al. [32])
- less oxidation in the reheating furnace and after rolling, with this a higher efficiency in the pickling line
- reduced oxidation of the strips and wear of working roll due to the reduced rolling temperature
- reduced water consumption on the run-out table
- possibility to produce thin hot strip as well as wider formats
- improved strip flatness control by rolling and cooling on an transformed and homogeneous microstructure

- reduction of subsequent cold rolling passes

Disadvantage of Ferritic Rolling

- In conventional rolling, roughing rolling requires higher rolling load due to the reduced rolling temperature. Herman and Leroy [36] attempts to use thin slab casting as initial material.

Low temperature slab reheating (1050-1150 °C) is applied to ferritic rolling, which leads to partial dissolution of precipitates after reheating and consequently easier to receive the recrystallized strip during coiling.

For the production of non aging, soft and fully recrystallized ferritic hot strips, a constant high coiling temperature must be performed to ensure full recrystallization of the entire length of the coils. This condition cannot be easily performed, when rolling strips with a thickness of lower than 1.5 mm, particularly in processing of IF steels. Partially strained microstructures are observed so that a subsequent annealing treatment is needed (Beco et al. [32]).

Cold rolling from ferritic rolled strip requires lower rolling force, torque and less reduction passes compared to cold rolling from austenitic rolled strip as shown in figure 2-17.

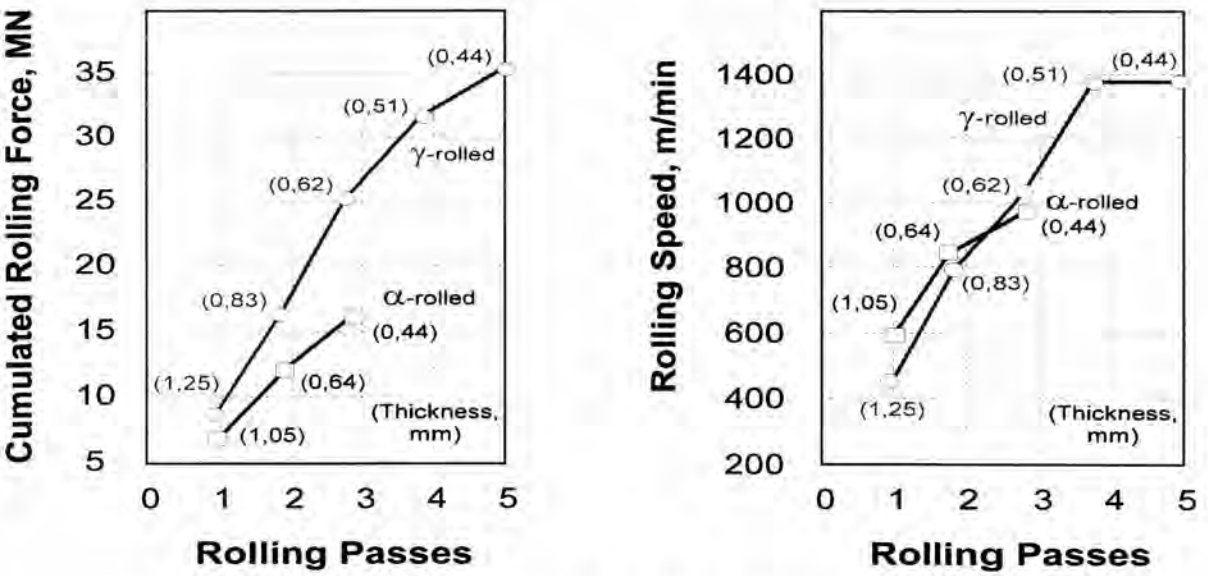

Fig. 2-17 : Process parameters for cold rolling (final thickness 0.44 mm) from austenitic or ferritic hot strip (Herman and Leroy [1])

Methods for Investigation of Hot Deformation Processes

In hot deformation simulation there is no suitable test method for general purpose since each method has a special field of application. There are many proper arguments for selecting a test method, but the important parameter is the metal forming process simulated (Lenard [37]). Additionally, the amount of deformation that can be applied without fracture of the sample (Moore [38]). In this work, hot deformation tests are used to determine flow curves and to evaluate deformed microstructure of specimens. This microstructure should be comparable to the microstructural evolution during hot rolling. Three basic test methods, tensile tests, compression tests and torsion tests are compared.

Tensile test is suitable for small strains. With higher strains above 0.7, this procedure becomes rather complex (Moore [38]). In torsion test, Backmann et al. [39] stated that the strain and strain rate distribution are not homogeneous; they are about zero on the axis and increase to maximum value at surface. For this work compression test is more suitable due to the same deformation mode as rolling concerning stress and strain distribution in the sample. Additionally, in hot compression tests, the use of lubricant is possible to obtain a homogeneous deformation. The advantages and disadvantages of those basic test methods are summarized in figure 2-18.

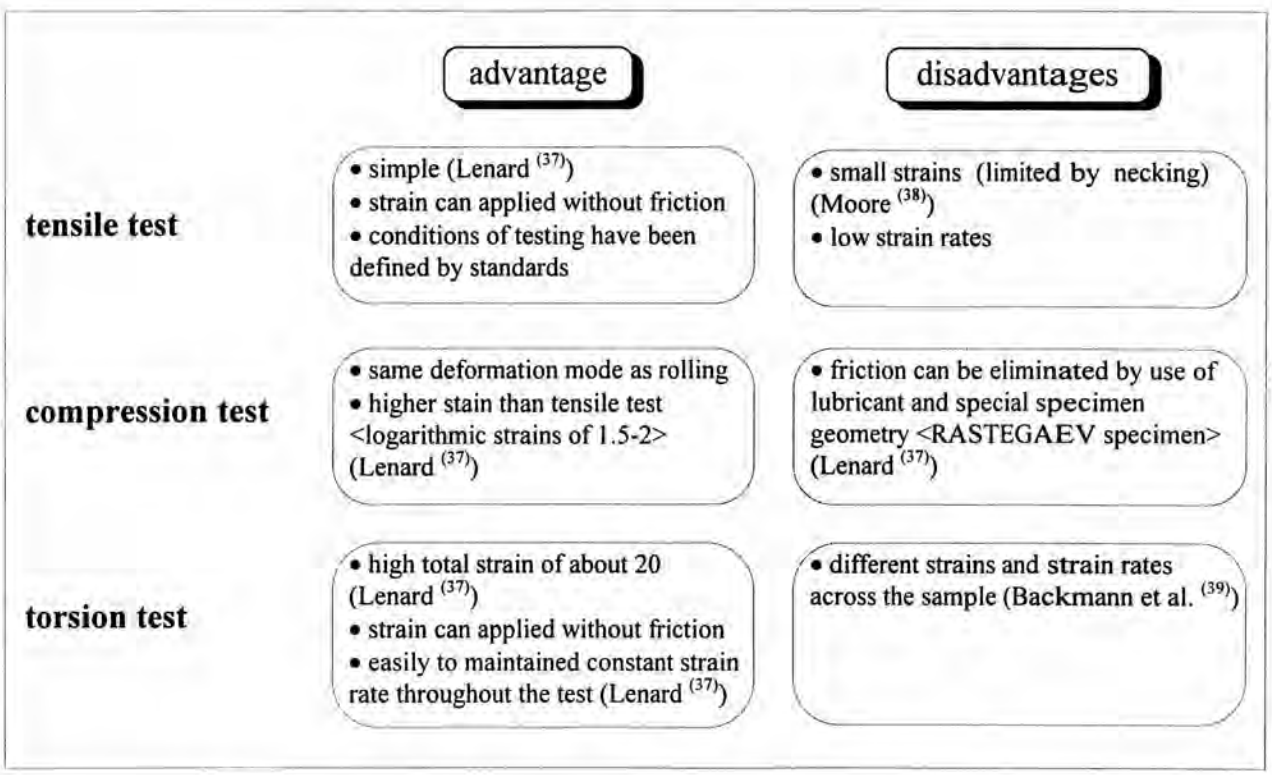

Fig. 2-18 : Comparison of hot deformation simulation methods

Hot Compression Test of Cylindrical Samples

Figure 2-19 illustrates the compression test of cylindrical specimen, where v is the deformation rate, F is the compressive load and h_0 and h are the initial and the instantaneous height of specimen.

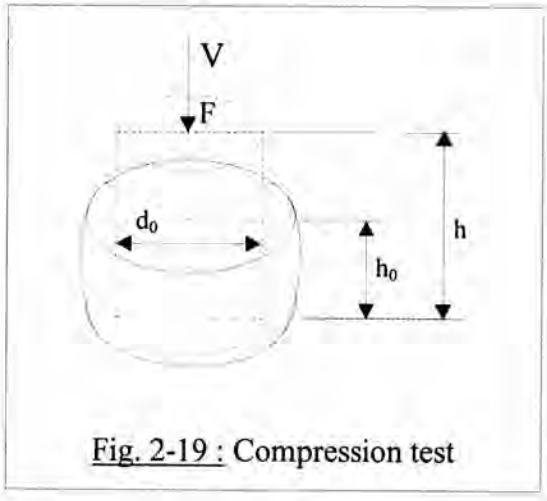

Fig. 2-19 : Compression test

The equivalent stress (σ_h) under load F is a function of cross section (A), which varies with the time. The equivalent stress can be expressed as

$$\sigma_h (t) = F(t)/[A_0 . (h_0 /h(t))] \qquad \text{(Equation 18)}$$

By using the parameters shown in figure 2-19, equation 18 can be written as follows

$$\sigma_h = \frac{4Fh}{\pi d_0^2 h_0} \qquad \text{(Equation 19)}$$

For both Tresca's and v. Mises's criterion the equivalent strain is given by

$$\varepsilon_h = \ln\left(\frac{h_0}{h}\right) \qquad \text{(Equation 20)}$$

The equivalent strain rate at the instantaneous height (h) of specimen is defined by

$$\dot{\varepsilon} = \frac{v}{h} \qquad \text{(Equation 21)}$$

Softening Flow Curves

In 1992, Jonas, Najafi-Zadeh and Yue [40] proposed the general relation between strain rate, temperature and flow stress, which can be expressed by the following equation

$$\dot{\varepsilon} = A\,[\sinh(\alpha\sigma)]^{a_{22}} \exp(-Q/RT) \qquad \text{(Equation 22)}$$

where A, α, a_{22} are constants and Q is the activation energy for hot deformation.

Jonas et al. also proposed that for strip rolling conditions (high stresses and relative low temperature), equation 22 can be reduced to an exponential relation as follows

$$\dot{\varepsilon} = B \exp(\beta\sigma)\exp(-Q/RT) \qquad \text{(Equation 23)}$$

where $\beta = \alpha n$. If σ_{mill} and σ_{lab} are the mean flow stresses at the strain rate $\dot{\varepsilon}_{mill}$ and $\dot{\varepsilon}_{lab}$, where $\dot{\varepsilon}_{mill}$ is defined as the hot strip mill strain rate and $\dot{\varepsilon}_{lab}$ is the simulation strain rate, at constant temperature equation 23 leads to the relation

$$\frac{\dot{\varepsilon}_{mill}}{\dot{\varepsilon}_{lab}} = \exp[\beta(\sigma_{mill} - \sigma_{lab})] \qquad \text{(Equation 24)}$$

or

$$\sigma_{mill} = \sigma_{lab} + a_{23} \log \frac{\dot{\varepsilon}_{mill}}{\dot{\varepsilon}_{lab}} \qquad \text{(Equation 25)}$$

where a_{23} is a constant.

From equation (25), the mean flow stress in the mill can approximately be calculated from the mean flow stress determined in simulation trials.